Experimental study on combustion pressure oscillation of soybean bio diesel oil

Ma Peng[1,3], Liu Huili[2], Liu Shengyong[3*]

(1. *Biomass Utilization Research and Development Center, Zhongzhou University, Zhengzhou 450044, China*;
2. *Students' Affairs Division, Zhengzhou Normal University, Zhengzhou 450044, China*;
3. *Key Laboratory of Renewable Energy Ministry of Agriculture, Henan Agricultural University, Zhengzhou 450002, China*)

Abstract: The principal objectives of this study were to examine in-cylinder combustion pressure oscillation characteristics of soybean biodiesel in time domain and time-frequency domain, and their influences on the control and operational parameters, such as injection timing, exhaust gas recirculation (EGR) ratio, engine load and engine speed. In this study, the combustion pressure oscillation characteristics of biodiesel engine for various injection timing, EGR ratio and engine speed were investigated. The corresponding relation of pressure characteristics in the time domain and frequency domain were obtained. The results showed that the pressure oscillation and peak pressure rise acceleration occurred mainly in the diffusion combustion, and the peak pressure rise rate located in the premixed combustion. The in-cylinder pressure level curve can be divided into three stages. The pressure levels of stage 1, stage 2 and stage 3 represent the peak in-cylinder pressure, the maximum amplitude of pressure rise rate and pressure rise acceleration, respectively. As the injection timing retards, the pressure levels of stage 1 and stage 3 decrease gradually. The pressure level curve of stage 3 with 25° before top dead center (BTDC) is the highest and the oscillation is the most significant. It is worth noting that the location of each stage with various operate conditions is not fixed. At 0.41 MPa indicated mean effective pressure (IMEP), with the increase of EGR rate, the pressure levels of stage 1 and stage 2 decrease gradually. The pressure level curve of stage 3 and the maximum amplitude of pressure rise acceleration with 0% EGR rate are the highest. The oscillation with 0% EGR rate is the most significant at 0.41 MPa IMEP. Compared to 0.41 MPa IMEP, the frequency bands of stage 1 and stage 2 at 1.1 MPa IMEP are relatively low due to the soft combustion in the cylinder. As EGR rate increases, the pressure level of stage 1 decreases, and those of stage 2 and stage 3 increase gradually. The oscillation with 30% EGR rate is the most significant. With the increase of engine speed, the pressure levels of stage 1 and stage 2 decrease, and move to the low frequency. The pressure level in the high frequency domain at 1600 r/min is less than that at 1100 r/min, and the combustion process is smooth.

Keywords: combustion pressure oscillation, soybean biodiesel, injection timing, exhaust gas recirculation, engine speed
DOI: 10.3965/j.ijabe.20160906.1680

Citation: Ma P, Liu H L, Liu S Y. Experimental study on combustion pressure oscillation of soybean bio diesel oil. Int J Agric & Biol Eng, 2016; 9(6): 156－166.

1 Introduction

Common rail direct injection diesel engine has the advantages of high injection pressure and flexible injection parameters, such as the injection timing, injection pressure and injection quantity. Compared to the traditional direct injection diesel engines, ignition delay is shorter and the ignition location at the front of the spray, so the combustion process is different[1]. Wang et al.[2] investigated the effects of injection timing and injection pressure on fuel economy and emission characteristics. The results demonstrated that increasing the injection pressure could improve fuel economy and smoke emission, but NOx was deteriorated. However, with very high injection pressure, the improving trends of smoke and fuel economy were not obvious, and even at

Received date: 2015-01-13 **Accepted date:** 2016-04-18
Biographies: Ma Peng, PhD, Associate Professor, research interests: the application and management of biomass energy, Email: mp@zhzhu.edu.cn; **Liu Huili**, Master, Lecture, research interests: the application and management of biomass energy, Email: 750023420@qq.com.
***Corresponding author: Liu Shengyong**, PhD, Professor, research interests: the application of biomass energy. Key Laboratory of Renewable Energy Ministry of Agriculture, Henan Agricultural University, Zhengzhou 450002, China. Tel: +86-13938488718, Fax: +86-371-68229609, Email: 76968418@qq.com.

low load condition, the economy would decline. With the delay of injection timing, NOx was reducd while smoke and fuel economy was augmented at high load. However, at the low load, smoke and NOx would decline simultaneously.

Herfatmanesh et al.[3] investigated the effects of fuel injection characterization on diesel combustion and emissions with two-stage fuel injection. The results indicated that two-stage injection had the potential for simultaneous reduction of NOx and soot emissions. Nevertheless, the studied two-stage strategies resulted in higher soot emission, mainly due to the interaction between two consecutive fuel injection events, whereby the fuel sprays during the second injection were injected into burning regions, generating fuel-rich combustion.

Agarwal et al.[4] investigated the effects of injection parameters, especially fuel injection pressure and injection timing on particulate size and number distribution in diesel exhaust. The experimental results indicated that the particulate size-number concentration increased with the increase of engine load and it reduced with the increase of fuel injection pressure.

An investigation of the impact of injection strategy on NOx and particulate matter (PM) emissions was conducted with a common-rail turbocharged diesel engine. It was found that at all load conditions; an increase of fuel injection pressure significantly increased NOx emissions. The results confirmed that the dominant factor that determined NOx emissions were the ignition event controlled by the oxygen equivalence ratio at the autoignition zone[5].

Abdullah et al.[6] investigated the effects of a variation of pilot injection timing with EGR on NOx emissions and soot emissions on a modern V6 common rail diesel engine. The results showed that the early pilot injection timing contributed to the lower soot level and higher NOx emissions. The higher level of NOx was due to higher combustion temperatures resulting from the complete combustion. Meanwhile, the lower soot level was due to complete fuel combustion and soot oxidation. The early pilot injection timing produced an intermediate main ignition delay which also contributed to complete combustion. The formation of smoke was higher at a high engine load than that at a low engine load due to the higher amount of fuel being injected.

Emissions characteristics of common-rail direct injection diesel engine have been widely investigated in recent studies. However, few research works focused on the in-cylinder combustion pressure oscillation characteristics, especially combustion pressure oscillation characteristics of engines fueled with biodiesel. The in-cylinder pressure is an important signal reflecting the combustion state and the direct excitation source of combustion noise. The study of Cerda et al.[7] showed that the main energy of combustion noise was derived from the combustion pressure oscillations. However, the oscillation energy was only about 5% of the total energy of the cylinder pressure. The engine vibration was excited by the high frequency pressure oscillation, and the acoustic energy was radiated outward which had an important contribution to combustion noise[8]. The analysis of pressure data in time domain and frequency domain, is able to provide insights into the efficiency and reliability of an biodiesel engine operation[9,10]. Peak pressure, peak pressure rise rate and peak pressure rise acceleration are the most commonly investigated[11-13]. An in-cylinder pressure-based control method is capable of improving engine performance, as well as reducing harmful emissions[14-16]. Compared to conventional petrol-diesel fuel, biodiesel can also enhance biodegradability, reduce toxicity and improve lubricity. The principal objectives of this study were to examine in-cylinder combustion pressure oscillation characteristics of soybean biodiesel in time domain and time-frequency domain, and the influences of the control and operational parameters, such as injection timing, exhaust gas recirculation (EGR) ratio, engine load and engine speed. The pressure oscillation transfer characteristics, the corresponding relation of pressure characteristics in the time domain and frequency domain of soybean biodiesel were also investigated.

2 Materials and methods

The combustion experiments in this study were performed on a turbo-charged in-line six-cylinder, direct injection heavy diesel engine with common rail injection.

The specifications of the engine and the experimental apparatus are shown in Table 1 and Figure 1, respectively. The engine was coupled to an electronically controlled hydraulic dynamometer. In the experiment, there were not any modifications to the engine, and engine speed kept at 1100 r/min and 1600 r/min. The test fuels were soybean biodiesel. The physical and chemical properties of the test fuels are given in Table 2. The EGR ratio was adjusted at 0%, 10% and 30% by controlling the EGR valve and EGR ratio was calculated at the ratio of CO_2 concentration between intake and exhaust gases.

Table 1 Specifications of base engine

Number of cylinders	In-line 6 cylinders
Bore×stroke/mm	126×155
Compression ratio	17:1
Engine displacement/L	11.596
Rated power/kW	353
Rated speed/r·min^{-1}	2100
Nozzle orifice number×diameter/mm	8×0.217

Table 2 Properties of test fuels

	Diesel	Soybean biodiesel
Density@20°C/kg·m^{-3}	834	883
Viscosity@40°C/mm^2·s^{-1}	2.48	4.51
Cetane Number	45	61
Lower Heating Value/MJ·kg^{-1}	42.53	37.47
Carbon Percentage/wt%	87.4	77.91
Oxygen Percentage/wt%	0	10.19

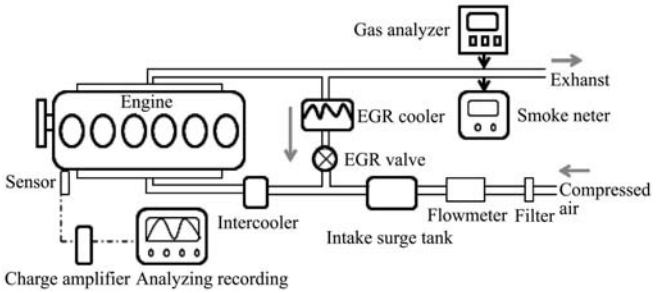

Figure 1 Experimental apparatus

In-cylinder pressure was measured by a Kistler (6125A) piezoelectric transducer, a Kistler (5015A) charges amplifier and a Yokogama (DL750) data analyzing recording. The pressure rise rate was calculated according to the sampled in-cylinder pressure. The heat release rate (HRR) was computed using the traditional first-law heat-release model.

In-cylinder pressure data analysis is the most effective method to analyze engine combustion behavior because it directly influences combustion characteristics. In this research, the combustion state of common rail biodiesel engine was evaluated. The pressure oscillation characteristics in the time domain were investigated by analyzing in-cylinder pressure, pressure rise rate, heat release rate and pressure rise acceleration with respect to crank angle. The pressure characteristics in the frequency domain were further investigated using the Fast Fourier Transform (FFT) and the corresponding characteristics relation in the time domain and frequency domain was determined. The frequency transfer characteristics with different injection timing, exhaust gas recirculation (EGR) ratio, engine load and engine speed were investigated, respectively. The peak value and phase in the time domain of in-cylinder pressure curve, the frequency structure of in-cylinder pressure curve, the corresponding component of each frequency band were further investigated for optimizing and controlling the combustion state.

3 Results and discussion

The plot of experimental in-cylinder pressure oscillation cycle is illustrated in Figure 2. It can be seen clearly that the serrated pressure fluctuation near the peak of the pressure curve in rough combustion. In normal combustion, the pressure curve increases smoothly to its peak, and then progressively decreases. The pressure curve of oscillation can be regarded as superposition of the smooth curve and oscillation curve. The smooth curve represents the primary energy of the combustion, and distributes in the low frequency domain. The pressure oscillation distributes in the high frequency domain, and represents the strong impact, which results in engine vibration and noise[17-19].

Figure 3 shows the plot of in-cylinder pressure, pressure rise rate, pressure rise acceleration and heat release rate, and their phase relationships have been identified. The pressure oscillation occurs mainly in the diffusion combustion, and peak in-cylinder pressure occurs after the peak of the premixed combustion. The peak pressure rise rate is located in the premixed combustion and peak pressure rise acceleration is in

diffusion combustion, respectively. The pressure oscillation and peak pressure rise rate is not in the same region. It means that the pressure rise rate cannot be fully representative of the pressure oscillations like pressure rise acceleration.

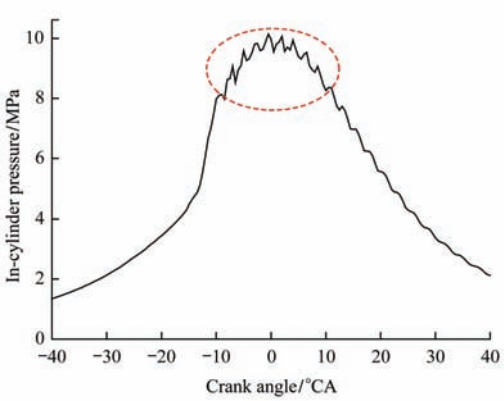

Figure 2 Plot of experimental in-cylinder pressure oscillation cycle

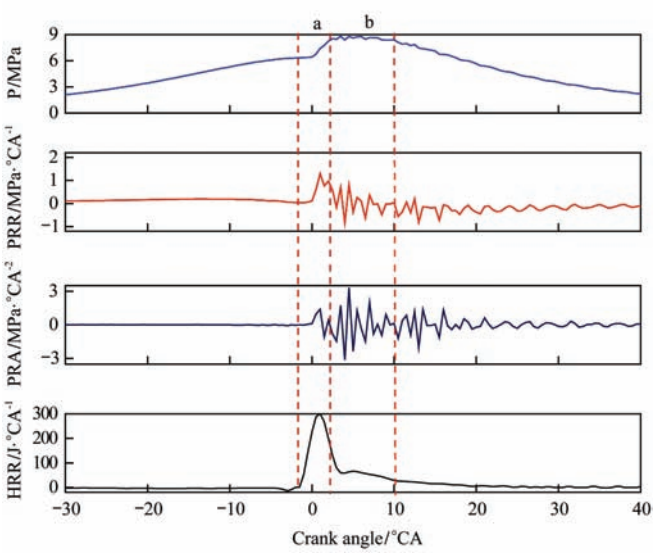

Figure 3 Plot of in-cylinder pressure, pressure rise rate, pressure rise acceleration and heat release rate

Figure 4 illustrates the effect of injection timing on in-cylinder pressure, heat release rate, and pressure rise rate and pressure rise acceleration. The engine speed is kept at 1600 r/min and the indicated mean effective pressure (IMEP) is 0.41 MPa. As the injection timing retards from 25° before top dead center (BTDC) to 5° BTDC and then to 0° BTDC, the peak pressure gradually decreases and its phase retards. The value is 10 MPa at 0.5°CA BTDC, 8.8 MPa at 3.5°CA ATDC and 8.5 MPa at 8°CA ATDC, respectively. In the analysis of heat release rate, with the retarding of injection, the peak of premixed combustion decreases first and then decrease, its phase retards gradually. The similar results are achieved in the Figure 4b the pressure rise rate. The maximum amplitude is 1.2 MPa/°CA, 1.3 MPa/°CA, 2 MPa/°CA, respectively. In the analysis of the pressure rise acceleration curves, the results are different. With the retarding of injection, the maximum amplitude of pressure rise acceleration increases first and then decreases, it is 6.4 MPa/°CA^2, 6.4 MPa/°CA^2, 5.5 MPa/°CA^2.

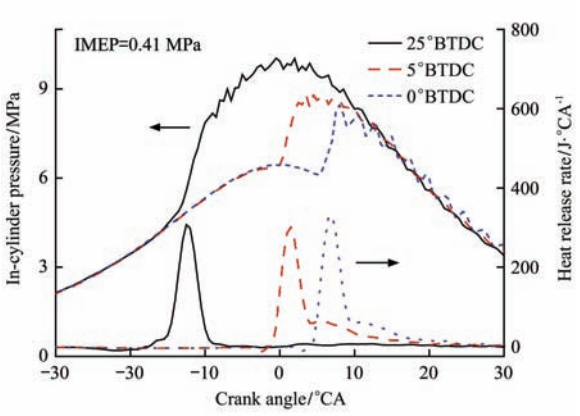

a. In-cylinder pressure and heat release rate

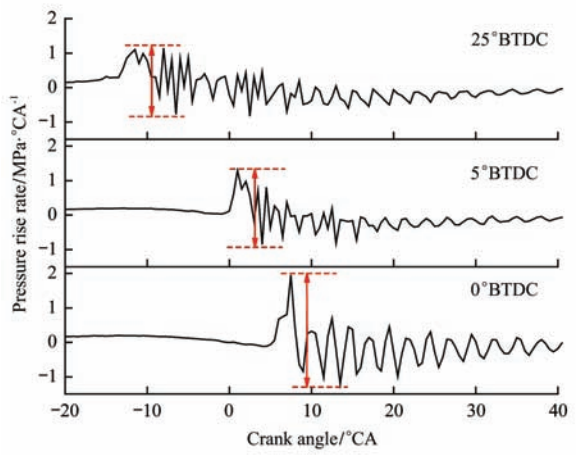

b. Pressure rise rate

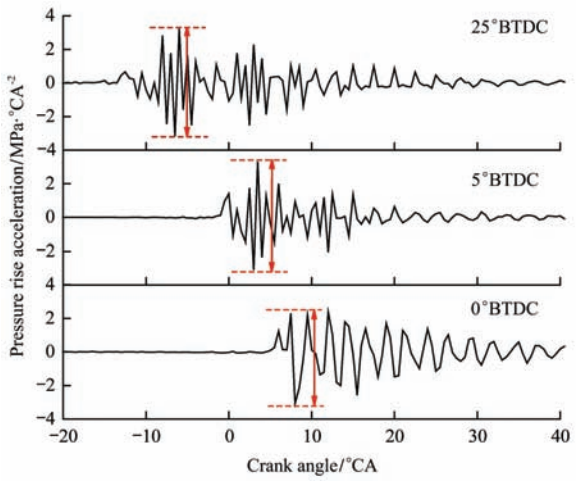

c. Pressure rise acceleration

Figure 4 Effects of injection timing on in-cylinder pressure, heat release rate, pressure rise rate and pressure rise acceleration

With 25° BTDC injection timing, the premixed combustion is the dominant and diffusion combustion is not obvious. As the injection timing retards from 25° BTDC to 5° BTDC, the in-cylinder temperature increase, so the premixed combustion decreases and the diffusion combustion increases, and pressure rise rate decreases. When injection timing is retarded to 0° BTDC, the combustion occurs during the expansion stroke, the in-cylinder temperature becomes lower, ignition delays, which lead to higher fuel proportions burning in the premixed combustion, so the peak of premixed combustion increases and pressure rise rate increases. It is noteworthy that the maximum amplitudes of pressure rise acceleration with 25° BTDC and 5° BTDC is close. The former is due to the higher proportion premixed combustion, and the latter is due to the combustion near the TDC.

The in-cylinder pressure with different injection timing was analyzed using FFT, and the results are shown in Figure 5. The characteristic parameters associated with the combustion process can be achieved according to the in-cylinder pressure level curve. The in-cylinder pressure level curve can be separated into three stages. In the low frequency band, the in-cylinder pressure level is higher, and there is a rapid pressure level drop (indicated as 1, 0-0.4 kHz). Then, it can be seen clearly that the pressure level drops slowly in the middle frequency band (indicated as 2, 0.4-2.2 kHz). In the high frequency band, the pressure level drops wave upon wave and decays off (indicated as 3, 2.2-10 kHz). Figure 5b shows the relation of pressure level in stage 1 and in-cylinder pressure in the time domain. As the injection timing retards from 25° BTDC to 0° BTDC, both the pressure level of stage 1 and the peak pressure decrease gradually. The pressure level of stage 1 represents the peak in-cylinder pressure and its duration. The greater the peak in-cylinder pressure, the greater the pressure level in stage 1. The shorter the duration of peak in-cylinder pressure, the faster the pressure level drops. Figure 5c shows the relationship between pressure level of stage 2 and pressure rise rate in time domain. As the injection timing retards from 25° BTDC to 0° BTDC, both the pressure level of stage 2 and the maximum amplitude of pressure rise rate increase gradually. The pressure level of stage 2 represents the maximum amplitude of pressure rise rate. The greater the maximum amplitude of pressure rise rate, the greater the pressure level of stage 2.

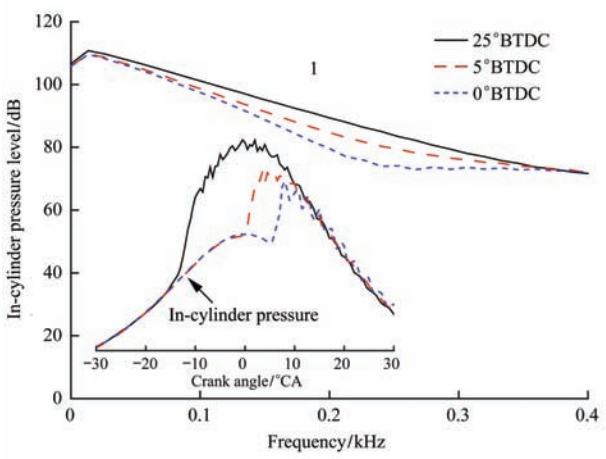

a. 0-10 kHz

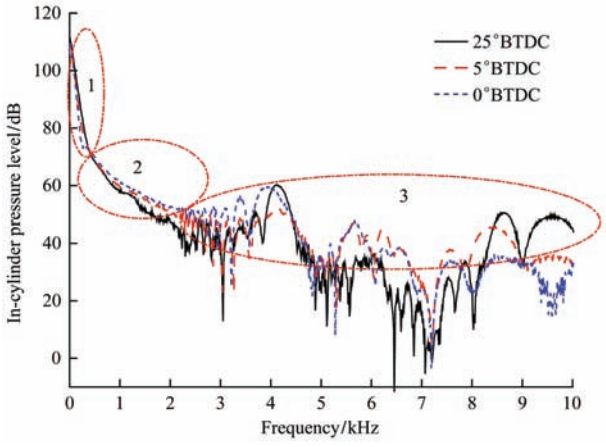

b. 0-0.4 kHz

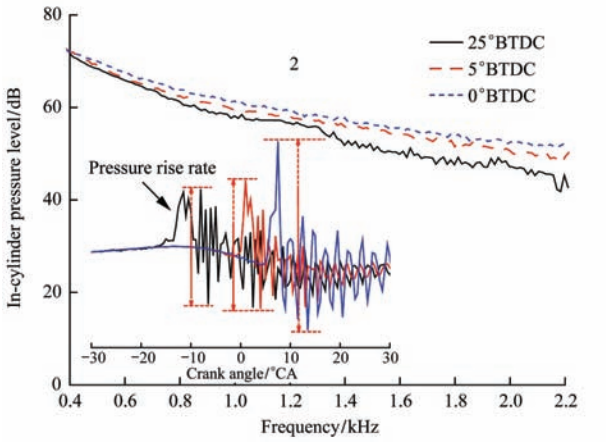

c. 0.4-2.2 kHz

Figure 5 FFT analysis of the in-cylinder pressure with different injection timing

There are several peaks in the pressure level curve of stage 3, which are caused by the high frequency pressure oscillation. The high peak means the intense pressure oscillations. The higher the pressure level curve of stage 3, the higher the pressure rise acceleration. It can be seen clearly that the pressure level curve of stage 3 with

25° BTDC is the highest and the oscillation is the most significant. It is in line with the conclusions of the Figure 4c, the maximum amplitude of pressure rise acceleration with 25° BTDC is the highest.

Figure 6 illustrates the effects of EGR rate on the in-cylinder pressure, heat release rate, pressure rise rate and pressure rise acceleration at 0.41 MPa IMEP.

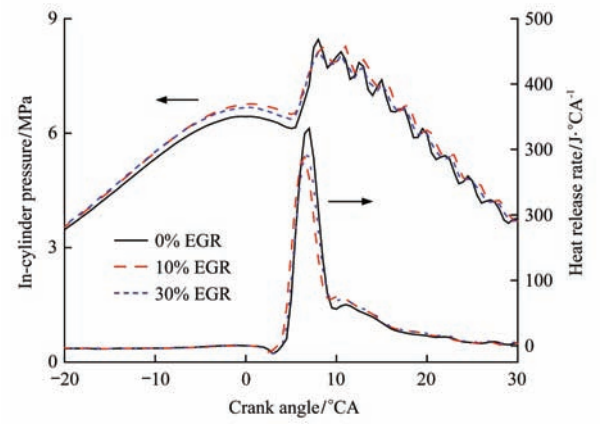

a. In-cylinder pressure and heat release rate

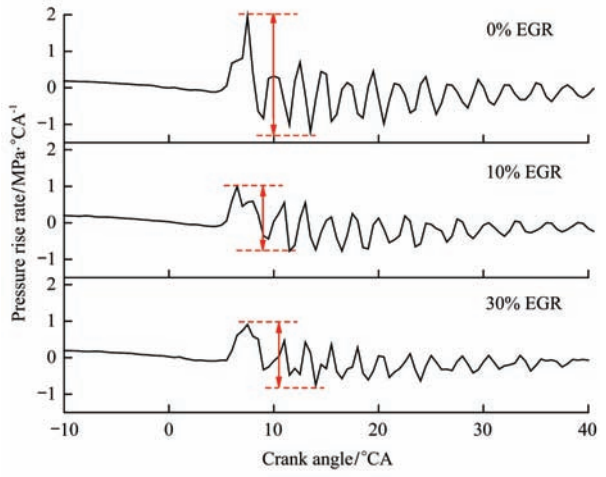

b. Pressure rise rate

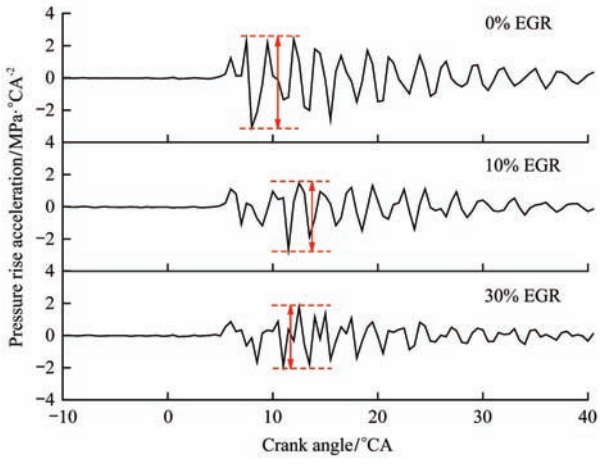

c. Pressure rise acceleration

Figure 6 Effects of EGR rate on the in-cylinder pressure, heat release rate, pressure rise rate and pressure rise acceleration at 0.41 MPa IMEP

The results show that, as EGR rate increase from 0 to 10% and 30%, the peak in-cylinder pressure decreases, the peak premixed combustion decreases and its phase advanced; the peak diffusion combustion increase. With the increase of EGR rate, both the maximum amplitude of pressure rise rate and pressure rise acceleration decreases, respectively. The maximum amplitude of pressure rise rate is 3.16 MPa/°CA, 1.77 MPa/°CA, and 1.67 MPa/^{o}CA, respectively. The maximum amplitude of pressure rise acceleration is 5.45 MPa/°CA^2, 4.11 MPa/°CA^2, and 3.67 MPa/°CA^2. The in-cylinder temperature is relatively low at the 0.41 MPa IMEP (low load). As EGR rate increases, the mean gas temperature in the cylinder increases, the ignition delay decreases, the combustion advances, so the fuel accumulated during the ignition delay period decrease, the peak premixed combustion and peak in-cylinder pressure decrease, and their phase advanced, respectively. The maximum amplitude of pressure rise rate and pressure rise acceleration decreases, respectively.

The effect of EGR rate on in-cylinder pressure level is illustrated in Figure 7. The overall trend of pressure level curves with different EGR rate is similar to Figure 5a. The overall process also can be divided into three stages. The in-cylinder pressure level drops fast in the low frequency band, and then becomes slow, and it drops wave upon wave and decays off in the high frequency band. It is worth noting that the frequency band of each stage is different to that in Figure 5 due to different combustion state in the cylinder. The frequency band of stage 1, 2 and 3 in Figure 7 is 0-0.3 kHz, 0.3-2.2 kHz and 2.2-10 kHz, respectively. The pressure level in stage 1 is correlated with in-cylinder pressure in time domain, and the results are shown in Figure 7b. With the increase of EGR rate, the pressure level in stage 1 decreases gradually, but the difference is not obvious. It is consistent with the trend of the in-cylinder pressure with different EGR rate. The relationship between pressure level of stage 2 and pressure rise rate in the time domain is shown in Figure 7c. As EGR rate increases, both the pressure level of stage 2 and pressure rise rate decrease. The maximum amplitudes of pressure rise rate with 10% and 30% EGR rate are similar and

significantly less than that with 0% EGR rate. The difference of pressure level curve with three EGR rates is completely consistent to that of pressure rise rate curves. The pressure level curves of stage 2 with 10% and 30% EGR rate are also close, and significantly less than that with 0% EGR rate.

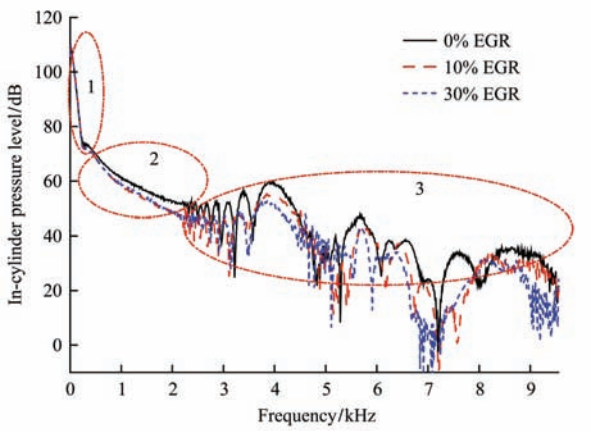

a. 0-10 kHz

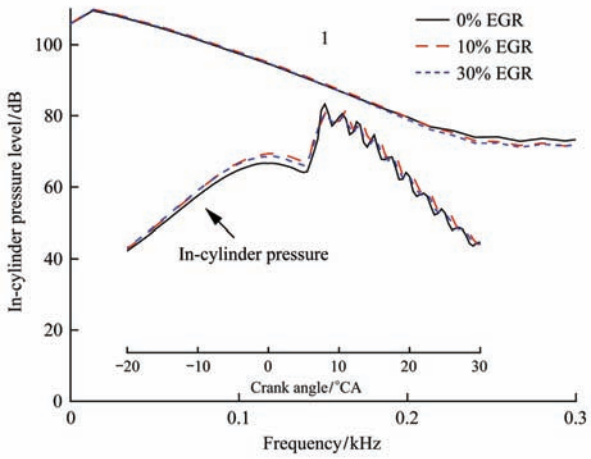

b. 0-0.3 kHz

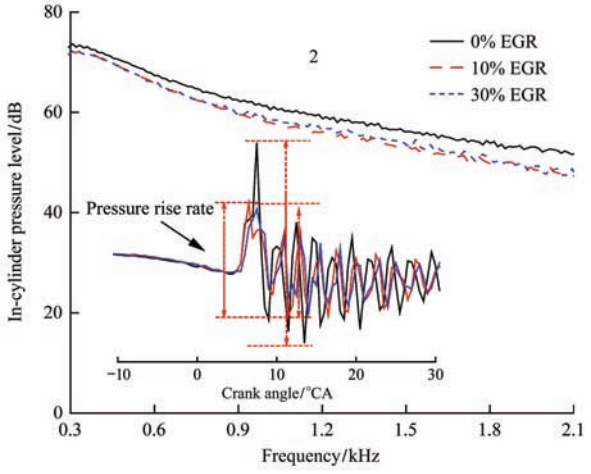

c. 0.3-2.2 kHz

Figure 7 FFT analysis of the in-cylinder pressure with different EGR rates at 0.38 MPa IMEP

Both the pressure level curve of stage 3 and the maximum amplitude of pressure rise acceleration with 0% EGR rate are the highest. It means that the oscillation with 0% EGR rate is the most significant. The in-cylinder temperature at 0.41 MPa IMEP is relatively low. As EGR rate increases, the temperature increases, the fuel accumulated during the ignition delay period decrease, the pressure rise acceleration decrease.

Figure 8 shows the effects of EGR rate on the in-cylinder pressure, heat release rate, pressure rise rate and pressure rise acceleration at 1.1 MPa IMEP.

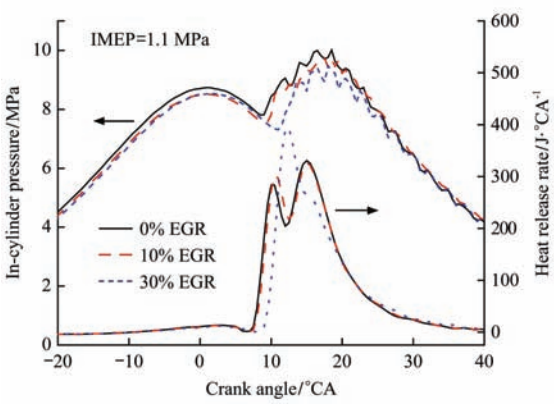

a. In-cylinder pressure and heat release rate

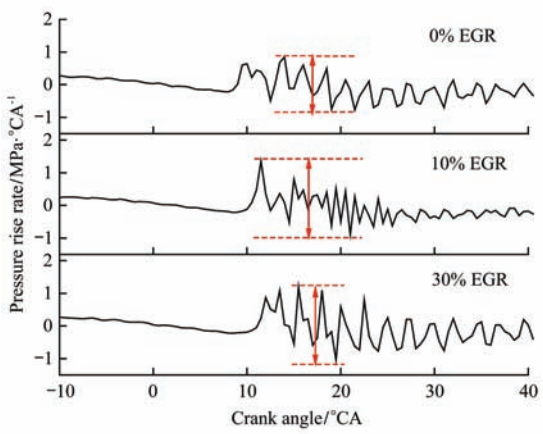

b. Pressure rise rate

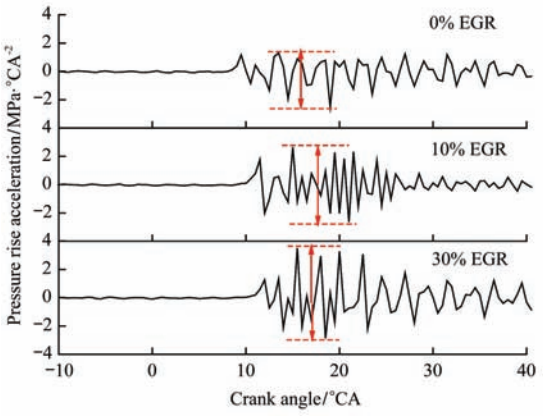

c. Pressure rise acceleration

Figure 8 Effects of EGR rate on the in-cylinder pressure, heat release rate, pressure rise rate and pressure rise acceleration at 1.1 MPa IMEP

With the increase of EGR rate, the peak in-cylinder pressure decreases, but the peak premixed combustion increases and its phase retards; the peak diffusion combustion decrease. As EGR rate increases, both the maximum amplitude of pressure rise rate and pressure rise acceleration increases. It is different with the results of 0.41 MPa IMEP in Figure 6. With the increase of EGR rate, the oxygen concentration decrease, the total specific heat capacity increase, so the mean temperature in the cylinder decrease, the ignition delay increases, the fuel accumulated during the ignition delay period increase, the peak premixed combustion, the maximum amplitude of pressure rise rate and pressure rise acceleration increase, and their phase retard.

Figure 9 illustrates the effects of EGR rate on the in-cylinder pressure level at 1.1 MPa IMEP. The pressure level drops first sharply then slowly and finally decays off in the high frequency domain. The frequency band of three stages is 0-0.2 kHz, 0.2-1.2 kHz and 1.2-10 kHz, respectively. Compared to the frequency band of stages 1, 2 at 0.41 MPa IMEP in Figure 7, the frequency band at 1.1 MPa IMEP is relatively low due to soft combustion in the cylinder. As EGR rate increases, the pressure level of stage 1 decreases and that of stage 2 increases gradually. The trend is in line with that of the in-cylinder pressure and pressure rise rate, respectively. As EGR rate increases, the pressure level of stage 3 increases. The maximum amplitude of pressure rise acceleration increases with the increase of EGR rate, as showed in Figure 8c. It proves the correlation of pressure rise acceleration and pressure level of stage 3 again.

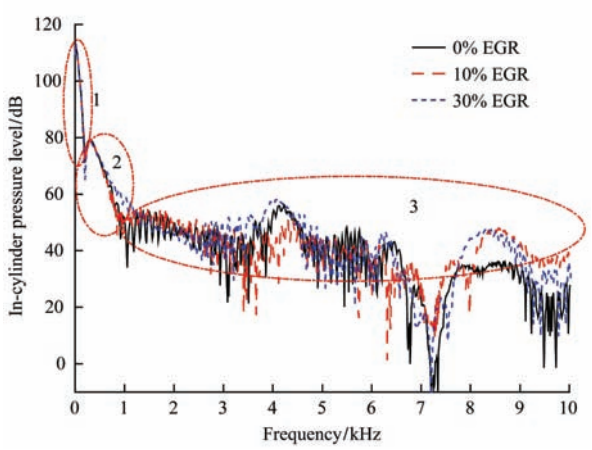

a. 0-10 kHz

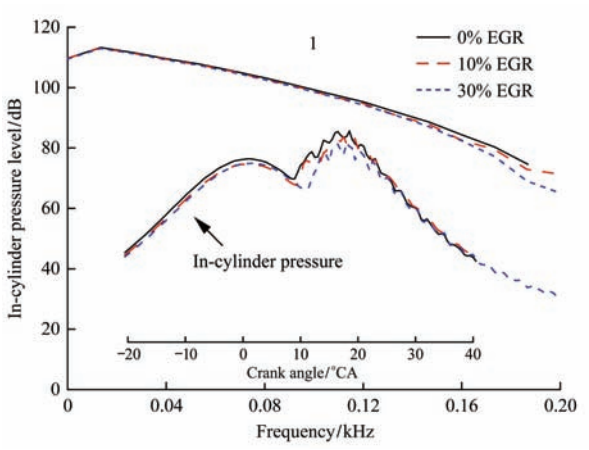

b. 0-0.2 kHz

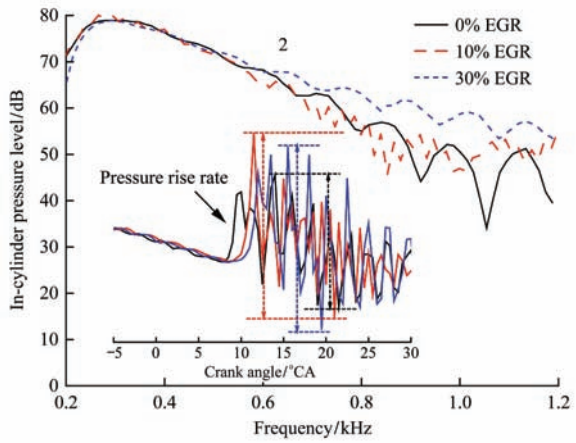

c. 0.2-1.2 kHz

Figure 9 FFT analysis of the in-cylinder pressure with different EGR rates at 1.1 MPa IMEP

The in-cylinder pressure, heat release rate, pressure rise rate and pressure rise acceleration with different engine speed are shown in Figure 10. The IMEP is 1.1 MPa, and the engine speed is 1100 r/min and 1600 r/min, respectively. As speed increases, the mean temperature in the cylinder increases, the ignition delay decreases, and the fuel accumulated during the ignition delay period decrease, so the peak in-cylinder pressure,

peak premixed combustion, the maximum amplitude of pressure rise rate and pressure rise acceleration decreases.

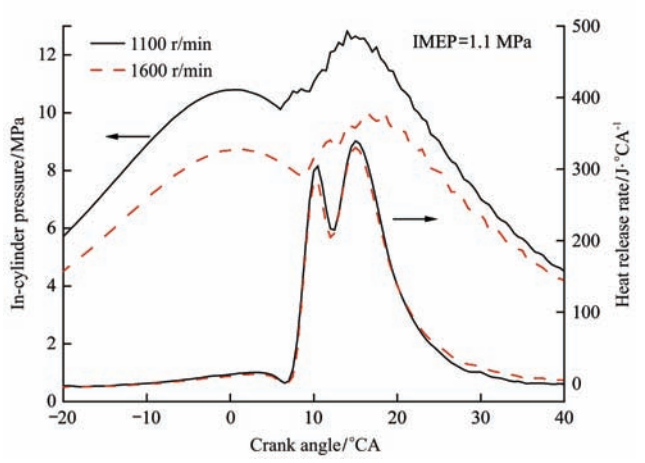

a. In-cylinder pressure and heat release rate

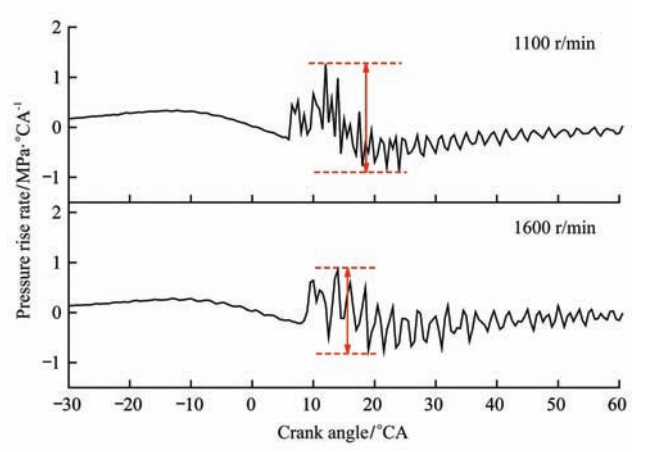

b. Pressure rise rate

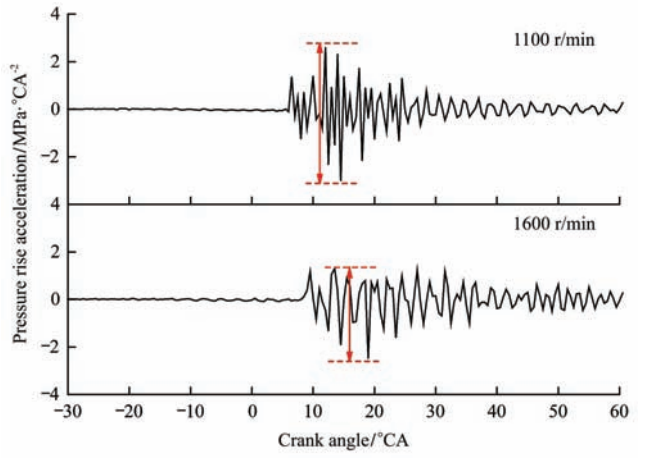

c. Pressure rise acceleration

Figure 10 In-cylinder pressure, heat release rate, pressure rise rate and pressure rise acceleration with different engine speeds

Figure 11 illustrates the effect of engine speed on the pressure level. The in-cylinder pressure level curve can also be separated into three stages. With the increase of engine speed, the pressure levels of stage 1 and stage 2 decrease, the stages 1 and stage 2 move to the low frequency. It is also consistent with the trend of in-cylinder pressure and pressure rise rate, respectively. The pressure level in the high frequency domain (stage 3) at 1600 r/min is lower than that at 1100 r/min, and the combustion is soft.

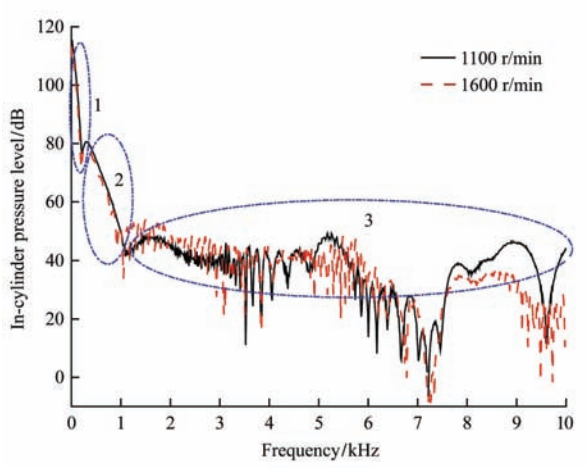

a. 0-10 kHz

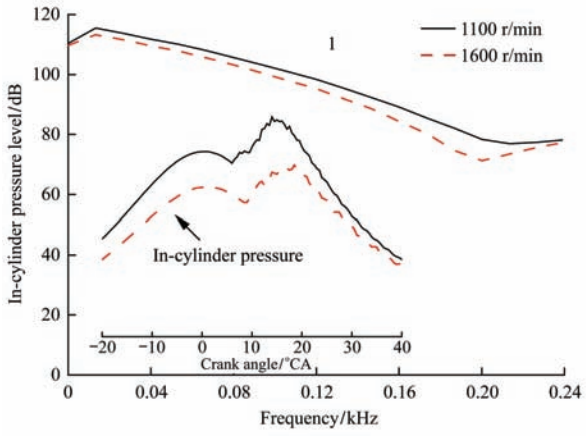

b. 0-0.24 kHz

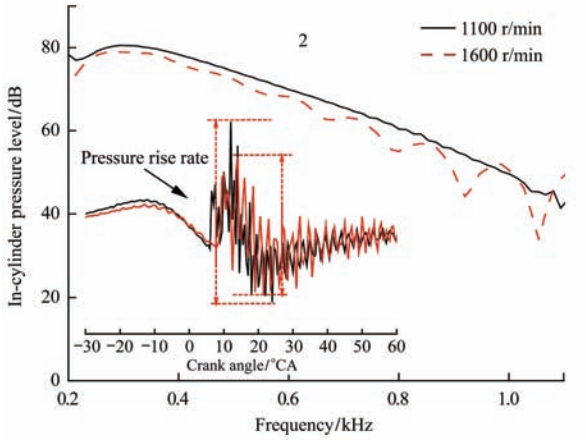

c. 0.2-1.1 kHz

Figure 11 FFT analysis of the in-cylinder pressure with different engine speeds

4 Conclusions

In this study, in-cylinder combustion pressure oscillation characteristics of soybean biodiesel in time domain and time-frequency domain, and the effects of the

injection timing, EGR ratio, engine load and engine speed on the characteristics were investigated. The corresponding relation of pressure characteristics in the time domain and frequency domain was also obtained.

(1) The pressure oscillation and peak pressure rise acceleration occur mainly in the diffusion combustion, and the peak pressure rise rate is located in the premixed combustion. The pressure oscillation and the peak pressure rise rate are not in the same region. It means that the pressure rise rate cannot be fully representative of the pressure oscillation like pressure rise acceleration.

(2) The in-cylinder pressure level curve can be divided into three stages. In stage 1, the in-cylinder pressure level is higher, and there is a rapid pressure level drop. Then, it can be seen clearly that the pressure level drops slowly in stage 2. In stage 3, the pressure level drops wave upon wave and decays off. The pressure level of stage 1 represents the peak in-cylinder pressure and its duration. The greater the peak in-cylinder pressure, the greater the pressure level in stage 1. The shorter the duration of peak in-cylinder pressure, the faster the pressure level drops. The pressure level of stage 2 and stage 3 represents the maximum amplitude of pressure rise rate and pressure rise acceleration, respectively. The greater the maximum amplitude, the greater the pressure level of stage 2 and stage 3.

(3) As the injection timing retards, the pressure level of stage 1 and stage 3 decreases, and the pressure level of stage 2 increase gradually. The pressure level curve of stage 3 with 25° BTDC is the highest and the oscillation is the most dramatic.

(4) It is worth noting that the location of each stage with various operate conditions are not fixed. At 0.41 MPa IMEP, with the increase of EGR rate, the pressure level in stage 1 decreases gradually, but the difference is not obvious. It is consistent with the trend of the in-cylinder pressure with different EGR rate. As EGR rate increases, both the pressure level of stage 2 and pressure rise rate decrease. The pressure level curve of stage 3 and the maximum amplitude of pressure rise acceleration with 0% EGR rate are the highest. It means that the oscillation with 0% EGR rate is the most dramatic.

(5) Compared to 0.41 MPa IMEP, the frequency bands of stage 1 and stage 2 at 1.1 MPa IMEP are relatively low due to the soft combustion in the cylinder. As EGR rate increases, the pressure level of stage 1 decreases and those of stage 2 and stage 3 increase gradually. The oscillation with 30% EGR rate is the most significant.

(6) With the increase of engine speed, the pressure levels of stage 1 and stage 2 decrease, and move to the low frequency. The pressure level in the high frequency domain at 1600 r/min is lower than that at 1100 r/min, and the combustion is soft.

Acknowledgements

This work was supported by The key scientific research project of Henan Province universities and colleges in 2017 (No. 17A630066); Public welfare industry (agriculture) special scientific research project-integration and demonstration of crop straw energy efficient and clean utilization technology research and development (No. 201503135); The youth core teacher training program of Henan Province universities and colleges in 2016.

The authors wish to thank Key Laboratory of Renewable Energy Ministry of Agriculture, Henan Agricultural University for their technical and financial support.

[References]

[1] Wang J X, Yang L, Xiao W Y, Liang F, Tan W C, Miao X J, et al. Influence of injection parameters on the performance of a DI diesel engine with GD-1 fuel injection system. Chinese Internal Combustion Engine Engineering, 2004; 25(2): 28–31. (in Chinese with English abstract)

[2] Tan X G, Sang H L, Tao Q. The impact of common rail system's control parameters on the performance of high-power diesel. Energy Procedia, 2012; 16: 2067–2072.

[3] Herfatmanesh M R, Lu P, Attar M A, Zhao H. Experimental investigation into the effects of two-stage injection on fuel injection quantity, combustion and emissions in a high-speed optical common rail diesel engine. Fuel, 2013; 109(7): 137–147.

[4] Agarwal A K, Dhar A, Srivastava D K, Maurya R K, Singh A P. Effect of fuel injection pressure on diesel particulate size and number distribution in a CRDI single cylinder research

engine. Fuel, 2013; 107(9): 84–89.

[5] Ye P, Boehman A L. An investigation of the impact of injection strategy and biodiesel on engine NOx and particulate matter emissions with a common-rail turbocharged DI diesel engine. Fuel, 2012; 97(7): 476–488.

[6] Abdullah N R, Mamat R, Wyszynski M L, Tsolakis A, Xu H. Effects of pilot injection timing and EGR on a modern V6 common rail direct injection diesel engine. 2013 IOP Conf. Ser.: Mater. Sci. Eng. 50012008.

[7] Cerda S, Romero J, Navasquillo J, Zurita J. A new time-frequency representation: Analysis of the combustion noise. Acta Acustica United with Acustica, 2001; 87(3): 423–425.

[8] Hou J X, Qiao X Q, Wang Z, Liu W, Huang Z. Characterization of knocking combustion in HCCI DME engine using wavelet packet transform. Applied Energy, 2010; 87(4): 1239–1246.

[9] Bodisco T, Reeves R, Situ R, Brown R. Bayesian models for the determination of resonant frequencies in a DI diesel engine. Mechanical Systems and Signal Processing, 2012; 26(1): 305–314.

[10] Hou J X, Qiao X Q, Wang Z, Liu W. Study on combustion stability of a DI-HCCI engine fueled with dimethyl ether. Journal of the Energy Institute, 2010; 83(2): 63–68.

[11] Amann C A. Cylinder-pressure measurement and its use in engine research. SAE paper 852067.

[12] Heywood J B. Internal combustion engine fundamentals. McGraw-Hill, Inc., 1988.

[13] Randolph A L. Methods of processing cylinder-pressure transducer signals to maximize data accuracy. SAE Paper 900170.

[14] Oh S, Kim J, Oh B, Lee K, Sunwoo M. Real-time IMEP estimation and control using an in-cylinder pressure sensor for a common-rail direct injection diesel engine. J. Eng. Gas Turbines Power, 2011; 133(6): 831–844.

[15] Han D, Ickes A M, Assanis D N, Bohac S V. Attainment and load extension of high-efficiency premixed low temperature combustion with dieseline in a compression ignition engine. Energy Fuels, 2010; 24(6): 3517–3525.

[16] Han D, Ickes A M, Bohac S V, Huang Z, Assanis D N. Premixed low temperature combustion of blends of diesel and gasoline in a high speed compression ignition engine. Proc Combust Inst, 2010; 33(2): 3039–3046.

[17] Schneider M, Schmillen K, Pischinger F. Regularities of cylinder pressure oscillations and their effects on the combustion process and noise. Measurement, 1987; 2013: 2–15.

[18] Hou J, Wen Z, Jiang Z, Liu Y. Effects of premixed ratio on combustion characteristics of a homogeneous charge compression ignition-direct injection engine fueled with dimethyl ether. Journal of Renewable and Sustainable Energy, 2014, 6(1): 104–108.

[19] Maurya R K, Pal D D, Agarwal A K. Digital signal processing of cylinder pressure data for combustion diagnostics of HCCI engine. Mechanical Systems and Signal Processing, 2013; 36(1): 95–109.